



# An empirical model of carbon flow through marine viruses and microzooplankton grazers

David Talmy <sup>1\*</sup>, Stephen J. Beckett <sup>2</sup>,  
Darcy A. A. Taniguchi,<sup>3</sup> Corina P. D. Brussaard,<sup>4</sup>  
Joshua S. Weitz<sup>2,5</sup> and Michael J. Follows<sup>6</sup>

<sup>1</sup>Department of Microbiology, University of Tennessee-Knoxville, Knoxville, TN, USA.

<sup>2</sup>School of Biological Sciences, Georgia Institute of Technology, Atlanta, GA, USA.

<sup>3</sup>Biology Department, California State University San Marcos, San Marcos, CA, USA.

<sup>4</sup>Department of Marine Microbiology and Biogeochemistry, Royal Netherlands Institute of Sea Research and University of Utrecht, Utrecht, the Netherlands.

<sup>5</sup>School of Physics, Georgia Institute of Technology, Atlanta, GA, USA.

<sup>6</sup>Department of Earth, Atmospheric and Planetary Sciences, Massachusetts Institute of Technology, Cambridge, MA, USA.

## Summary

**Viruses and microzooplankton grazers represent major sources of mortality for marine phytoplankton and bacteria, redirecting the flow of organic material throughout the world's oceans. Here, we investigate the use of nonlinear population models of interactions between phytoplankton, viruses and grazers as a means to quantitatively constrain the flow of carbon through marine microbial ecosystems. We augment population models with a synthesis of laboratory-based estimates of prey, predator and viral life history traits that constrain transfer efficiencies. We then apply the model framework to estimate loss rates in the California Current Ecosystem (CCE). With our empirically parameterized model, we estimate that, of the total losses mediated by viruses and microzooplankton grazing at the focal CCE site,  $22 \pm 3\%$ ,  $46 \pm 27\%$ ,  $3 \pm 2\%$  and  $29 \pm 20\%$  were directed to grazers, sloppy feeding (as well as excretion and respiration), viruses and viral lysate respectively. We identify opportunities to leverage**

**ecosystem models and conventional mortality assays to further constrain the quantitative rates of critical ecosystem processes.**

## Introduction

Viruses and microzooplankton grazers are major sources of phytoplankton mortality throughout the world's oceans (Fuhrman, 1999; Calbet and Landry, 2004; Evans and Brussaard, 2012; Mojica *et al.*, 2016; Våge *et al.*, 2018). However, quantification of impacts of these ecological interactions and the resulting fate of carbon remains challenging (Brussaard *et al.*, 2008; Weitz and Wilhelm, 2012; Brum *et al.*, 2015; Breitbart *et al.*, 2018). Viral lysis and grazing have potentially divergent consequences for the flow of carbon (Fig. 1). Grazing transfers carbon to higher trophic levels and may, in turn, catalyse the formation and aggregation of sinking organic particles. In contrast, lysis may favour the production of dissolved organic detritus (Wilhelm and Suttle, 1999), though viral lysis products may also aggregate and sink through the water column (Weinbauer, 2004; Guidi *et al.*, 2015). To quantify the relative importance of viral lysis and grazing and their respective impact on biogeochemical dynamics, it is essential to develop mechanistic biogeochemical models at regional and global scales.

The acquisition of quantitative data and characterizations of grazing and viral infection dynamics—and their consequences for carbon flow—remains challenging. One approach, the dilution method, has been routinely used for decades to estimate growth and mortality of primary and secondary producers (Landry and Hassett, 1982; Calbet and Landry, 2004). Modifications of the dilution method have been used to also estimate rates of mortality due to viral lysis (Evans *et al.*, 2003; Kimmance and Brussaard, 2010). Despite the significant assumptions that must be made (Dolan and McKeon, 2005; Beckett and Weitz, 2017, 2018), dilution experiments can provide critical sources of quantitative information on loss rates in marine microbial systems (Baudoux *et al.*, 2006).

Despite their potential, results from dilution experiments have had limited application to modelling material transfer mediated by viruses and microzooplankton grazers (Li *et al.*, 2011; Stukel *et al.*, 2011; Chen *et al.*, 2014). This

Received 9 August, 2018; revised 3 April, 2019; accepted 8 April, 2019. \*For correspondence. E-mail dtalmy@utk.edu; Tel. +1 617-800-3630

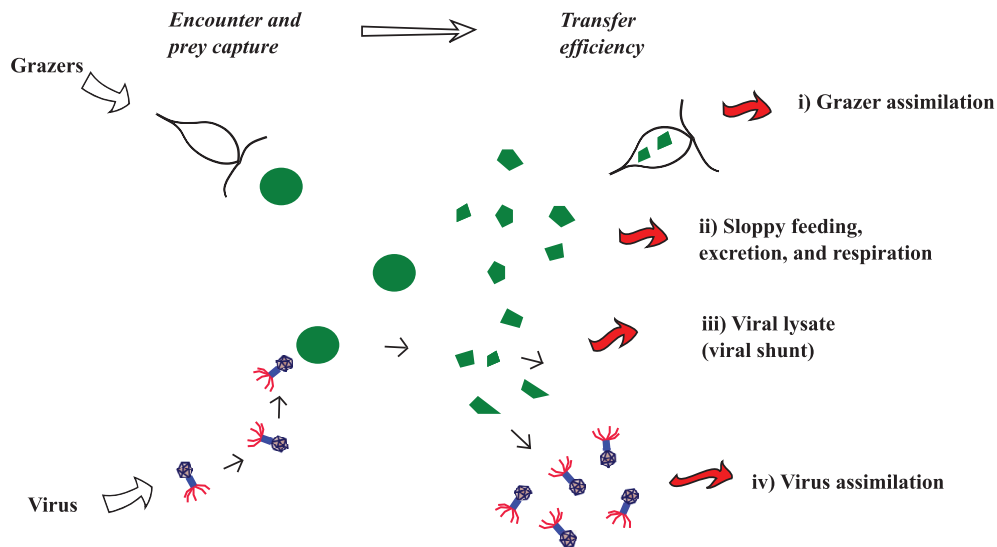


**Fig. 1.** Carbon fluxes from phytoplankton to viruses and microzooplankton grazers. The green circles represent a phytoplankton cell. The block and line arrows represent grazer and virus encounter with host cells due to motile behaviour and Brownian motion respectively. Green fragments represent organic matter and we do not differentiate between dissolved and particulate forms. Solid red arrows are key carbon fluxes: (i) assimilation into grazer biomass, (ii) grazing related losses to sloppy feeding, excretion and respiration, (iii) the 'viral shunt'; viral lysate directed towards detrital pools and (iv) assimilation into viral progeny. The goal of this work is to parameterize the four major carbon fluxes (i)–(iv) shown with large red arrows.

limitation is partly because dilution experiments provide information in the form of a system-specific loss rate, and require additional measurements to inform ecosystem model parameterization. Given appropriate auxiliary measurements, dilution experiments can provide constraints on parameterizations and parameter values that can be directly utilized in the ecosystem and biogeochemical models.

Here we demonstrate how, with appropriate additional measurements, we can provide constraints on carbon flows from phytoplankton to other major sinks including viruses, grazers, viral lysate and the combined sum of sloppy feeding, excretion and respiration (Fig. 1). We focus here on a study site in the California Current Ecosystem (CCE) (Pasulka *et al.*, 2015). The CCE offers prior *in situ* estimates of virus and grazer related mortality accompanied by concurrent measurements of virus abundance and microzooplankton carbon that are essential for the modelling approach presented here. As we will show, the integration of model-based analysis with appropriate datasets enable us to move towards estimates of carbon flow within marine microbial ecosystems.

### Parameterizing carbon flow

We describe parameters and constraints on phytoplankton rates of loss to viral lysis and grazing in mixed communities. We further consider additional information required to convert specific loss rates to fluxes depicted in Fig. 1.

### Nonlinear model of population dynamics

Consider the following mass balance equation for a population of phytoplankton  $P$ :

$$\frac{dP}{dt} = \underbrace{\mu P}_{\text{phyto-growth}} - \underbrace{m_v P}_{\text{viral lysis}} - \underbrace{m_z P}_{\text{grazing}} \quad (1)$$

In Eq. 1, producers grow at rate  $\mu$ . Specific loss rates due to grazing and viral infection are represented with  $m_z$  and  $m_v$  respectively. All parameters have units inverse time. Other producer losses exist, e.g. due to sinking or grazing by higher trophic levels, but are not included in Eq. 1. The focus of this work is to parameterize loss rates and fluxes that can be constrained with information from dilution experiments, where losses due to sinking and consumption by higher trophic levels are routinely removed (Evans *et al.*, 2003; Mojica *et al.*, 2016). Note that all parameters and variables are defined in Table 1. A detailed discussion of the assumptions used in the dilution technique is provided in Supporting Information Appendix S1A.

In Eq. 1, the loss terms  $m_v P$  and  $m_z P$  are the net flux from producers to viruses and grazers, including also flux to viral lysate, and detrital and inorganic carbon pools (Fig. 1). Equation 1 obtains flux estimates with knowledge of specific loss rates  $m_z$  and  $m_v$ , and phytoplankton biomass  $P$ . Specific loss rates due to grazer and virus-induced mortality ( $m_z$  and  $m_v$ ) can be estimated through

**Table 1.** Parameter and variable descriptions and units.

Symbol	Description	Units
$P$	Producer biomass density	$\mu\text{mol C l}^{-1}$
$V$	Virus biomass density	$\mu\text{mol C l}^{-1}$
$Z$	Grazer biomass density	$\mu\text{mol C l}^{-1}$
$\mu$	Producer growth rate	$\text{day}^{-1}$
$m_v$	Specific loss rate due to viral lysis	$\text{day}^{-1}$
$m_z$	Specific loss rate due to microzooplankton grazing	$\text{day}^{-1}$
$\phi_v$	Virus maximal carbon clearance rate	$\text{l } (\mu\text{mol C})^{-1} \text{ day}^{-1}$
$\phi_z$	Grazer maximal carbon clearance rate	$\text{l } (\mu\text{mol C})^{-1} \text{ day}^{-1}$
$\varepsilon_v$	Virus gross growth efficiency	–
$\varepsilon_z$	Grazer gross growth efficiency	–
$\beta$	Virus burst size	Viruses per cell
$Q_v$	Virus particle carbon quota	$\mu\text{mol C}$
$Q_h$	Host carbon quota	$\mu\text{mol C}$
$\delta_{vv}$	Quadratic virus mortality coefficient	$\text{l } (\mu\text{mol C})^{-1} \text{ day}^{-1}$
$\delta_{zz}$	Quadratic grazer mortality coefficient	$\text{l } (\mu\text{mol C})^{-1} \text{ day}^{-1}$

multiple methods, including the dilution method (Landry and Hassett, 1982; Calbet and Landry, 2004), and the modified dilution technique (Evans *et al.*, 2003; Kimmance and Brussaard, 2010). Estimates of  $m_z$  and  $m_v$  from these techniques lead to direct flux estimates for specific systems, but they cannot be used for prognostic ecosystem simulations that also describe and predict virus and microzooplankton community dynamics.

Consider again the phytoplankton mass balance model in Eq. 1, this time given mass–action losses due to infection and grazing:

$$\frac{dP}{dt} = \underbrace{\mu P}_{\text{phyto-growth}} - \underbrace{\phi_v VP}_{\text{viral lysis}} - \underbrace{\phi_z ZP}_{\text{grazing}} \quad (2)$$

where  $P$ ,  $V$  and  $Z$  are the microbial producer, virus and grazer carbon density respectively,  $\mu$  is the producer gross growth rate and  $\phi_z$  and  $\phi_v$  are microzooplankton and virus maximal carbon clearance rates respectively (Table 1). Zooplankton ecologists refer to the slope  $\phi_z$  as the maximal clearance rate, and for generality, we extend this terminology and define  $\phi_v$  as the viral maximal clearance rate. To link directly with carbon transfer rates, our clearance rates define the propensity for carbon transfer per unit biomass in the grazers and viruses. We refer to both rates as ‘maximal carbon clearance rates’ to distinguish them from per-capita equivalents (Kiørboe, 2011).

Equation 2 is the same mass balance as Eq. 1 with subtle yet important differences that we will compare and contrast. The loss rates  $m_z$  and  $m_v$  in Eq. 1 only apply to a single set of virus and grazer biomass densities—namely, those at the study site where the dilution technique was applied. Experimental values of  $m_z$  and  $m_v$  are therefore *system-specific*. Eq. 2 replaces system-specific loss rates

$m_z$  and  $m_v$  with the products  $\phi_z Z$  and  $\phi_v V$ , explicitly resolving the dependence of phytoplankton loss rate on virus and grazer biomass density. Maximal carbon clearance rates  $\phi_z$  and  $\phi_v$  control how virus and grazer biomass density influence phytoplankton loss rates, and are *process-specific* rates. Although rarely considered, dilution experiments that estimate *system-specific* loss rates  $m_z$  and  $m_v$  may also provide constraints on *process-specific* rates  $\phi_z$  and  $\phi_v$ , thereby contributing more directly to ecosystem model parameterization.

### Linking loss rates with fluxes

Only a portion of the phytoplankton losses due to viral lysis and grazing are actually incorporated into virus and grazer carbon biomass. We introduce transfer efficiencies  $\varepsilon_v$  and  $\varepsilon_z$  that represent the proportion of lost producer material that is incorporated into viruses and grazers respectively. The transfer efficiencies partition the flux from producers between each of the pools depicted in Fig. 1. If losses are characterized with Eq. 1, the fluxes incorporated into grazer and virus biomass are simply  $\varepsilon_z m_z P$  and  $\varepsilon_v m_v P$  respectively. These fluxes are sources of virus and grazer production, and are an important step towards understanding system dynamics. Also important are the associated fluxes towards dissolved and particulate pools,  $(1 - \varepsilon_z)m_z P$  and  $(1 - \varepsilon_v)m_v P$ . In Table 2, we summarize how the parameters  $\varepsilon_z$  and  $\varepsilon_v$  may be used in Eqs. 1 or 2 to quantify the flux of organic material from phytoplankton to the various fates depicted in Fig. 1. Our goal is to empirically constrain each of the parameters required to predict the fluxes in Fig. 1, focusing on the contrasting assumptions between the approximations taken directly from the dilution technique (Eq. 1), and model equivalents that explicitly resolve the dependence of fluxes on grazer and virus carbon density (Eq. 2). Particular attention is paid to the assumptions and measurements required to link the distinct approaches.

**Table 2.** Contrasting methods for calculating the flux of organic material from phytoplankton to microzooplankton grazers and viruses.

	Dilution technique approximation (Eq. 1)	Typical modelled flux (Eq. 2)
Flux to virus	$\varepsilon_v m_v P$	$\varepsilon_v \phi_v VP$
Flux to grazer	$\varepsilon_z m_z P$	$\varepsilon_z \phi_z ZP$
Flux to viral lysate	$(1 - \varepsilon_v)m_v P$	$(1 - \varepsilon_v)\phi_v VP$
Flux to sloppy feeding and respiration	$(1 - \varepsilon_z)m_z P$	$(1 - \varepsilon_z)\phi_z ZP$

Parameters and variables are defined in Table 1. In this work, we empirically constrain each of the terms and compare and contrast the different approximations.

### Empirical constraint on transfer efficiency

The gross growth efficiency (GGE) is a measure of the proportion of carbon ingested by grazers incorporated into biomass, after accounting for losses due to sloppy feeding, respiration and excretion. For grazers, estimates of GGE have been used to model carbon transfer (Taniguchi *et al.*, 2014). Here, we assume GGE is an empirical analogue of  $\epsilon_z$ . To compare and contrast virus and grazer transfer efficiency, we approximated  $\epsilon_v$  based on burst size ( $\beta_v$ ), virus particle carbon quota ( $Q_v$ ) and producer cell carbon quota ( $Q_h$ ; Jover *et al.*, 2014; Weitz, 2015):

$$\epsilon_v = \beta_v \frac{Q_v}{Q_h} \quad (3)$$

We compiled estimates of virus size, host size and burst size (Supporting Information Table S1). Using the allometric relations in Table 3, we estimated the virus GGE ( $\epsilon_v$ ) for a broad range of viruses, including cyanobacteriophage, viruses of eukaryotic algae, double-stranded DNA and double-stranded RNA viruses.

### Results and discussion

Our initial aim is to empirically constrain phytoplankton losses and the efficiency of transfer to viruses and higher trophic levels. The fluxes are listed in Table 2 and depicted in Fig. 1. We begin by presenting empirical findings of the transfer parameters  $\epsilon_z$  and  $\epsilon_v$ , and show how these may be combined with specific loss rates  $m_z$  and  $m_v$  from the CCE, to predict the fluxes in Fig. 1. We then present steps necessary to embed these parameters within an ecosystem model with explicit representation of feedbacks between phytoplankton, microzooplankton and virus dynamics. We discuss the application of this model for more general prediction of the fluxes in Fig. 1.

### Virus and grazer transfer efficiency

In Fig. 2, we show the relationship between virus radius, and virus carbon gross growth efficiency (GGE) estimated with Eq. 3. Also shown for comparisons are measured GGE for a range of grazer sizes, using the compilation of Taniguchi *et al.* (2014). Despite significant uncertainty, the comparison shows clearly that viral GGE ( $\epsilon_v$ ) is significantly lower than the grazer GGE ( $\epsilon_z$ ). This simple analysis suggests that compared to grazers, viruses do not assimilate a large portion of their hosts' carbon, consistent with prior findings (Jover *et al.*, 2014). The release of viral lysates leads to a carbon shunt from the particulate to the dissolved phase (Wilhelm and Suttle, 1999). To constrain the partition of material flux towards grazers, viruses and other sinks (Fig. 1), we also require rates of transfer.

### Carbon flow in a CCE

Consider again the carbon fluxes depicted in Fig. 1, and listed in Table 2. Since transfer efficiencies  $\epsilon_z$  and  $\epsilon_v$  can be estimated from laboratory experiments (Fig. 2), and loss rates  $m_z$  and  $m_v$  can be taken directly from dilution experiments (Supporting Information Table S2), these fluxes and associated uncertainties can be constrained. The model predicts that of the losses to grazers and viruses in the CCE,  $22 \pm 3\%$ ,  $46 \pm 27\%$ ,  $3 \pm 2\%$  and  $29 \pm 20\%$  are partitioned to grazer biomass, sloppy feeding (including respiration and excretion), viral biomass and viral lysate respectively (note that propagation of uncertainty in parameter estimates is described in the Supporting Information Appendix S1B). Thus, almost one-third of the phytoplankton carbon is lost to the viral shunt, with a relatively small portion going to viruses themselves. In contrast, approximately one-fifth of phytoplankton carbon is transferred to grazers. Overall, around 75% of the material is transferred to the detrital and inorganic carbon pools, through a combination of sloppy feeding, respiration and viral lysis. Some of this material may be retained in the surface ocean through regenerative

**Table 3.** Size-dependent carbon quotas for viruses and their hosts.

Trait	Parameterization	Comments
$Q_v$	$[41(r_v - 2.5)^3 + 130(7.5r_v^2 - 18.75r_v + 15.63)] / (1 \times 10^6) / (6.022 \times 10^{23})$	Constants were determined with a model of virus head structure, with literature values used to define key structural traits such as virus capsid thickness (Jover <i>et al.</i> , 2014). Note that the fitted values assume virus size (head radius, $r_v$ ) is expressed in nm.
$Q_h$	$\log_{10}(Q_h (1 \times 10^6) \cdot 12.0107) = [-0.538 \pm 0.158] + [0.86 \pm 0.06] \log_{10}(V)$	$V$ is cell volume ( $V = 4/3\pi r_h^3$ ), where $r_h$ is host equivalent spherical radius in $\mu\text{m}$ . Numerical values are from statistical fitting of relations between protist plankton ( $< 3000 \mu\text{m}^3$ ) cell carbon and volume (Menden-Deuer and Lessard, 2000)

Numerical values within square brackets are in the units originally reported, values outside square brackets, without errors, are conversions to  $\mu\text{mol C individual}^{-1}$ . Ranges correspond to 95% confidence intervals.

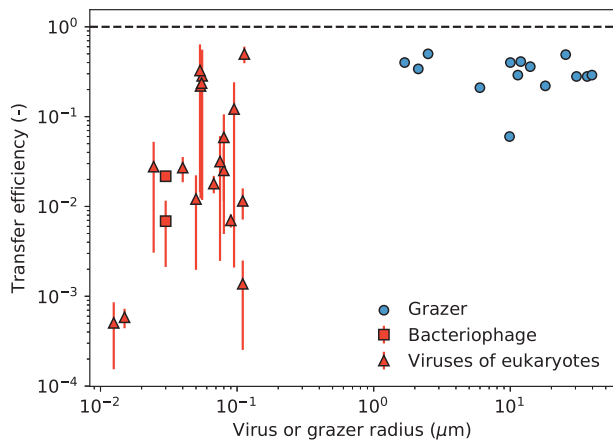


**Fig. 2.** Inferred virus gross growth efficiency (GGE;  $\epsilon_v$ , red squares and triangles) compared with grazer GGE ( $\epsilon_z$ , blue circles). The virus GGE was inferred using Eq. 3, where cell quotas were inferred using the allometric equations in Table 3 (sources are in Supporting Information Table S1). The microzooplankton GGE was taken directly from Taniguchi *et al.* (2014). Uncertainty ranges on virus GGE were calculated with upper and lower bounds of Eq. 3 based on values in Table 2. The horizontal dashed line marks 100% transfer efficiency. Median virus and grazer GGE are 0.023 and 0.315 respectively. Virus GGE is in general less than that of grazers.

mechanisms (Wilhelm and Suttle, 1999), and some may aggregate and be removed via sinking (Engel *et al.*, 2004; Laber *et al.*, 2018).

#### Towards ecosystem structure and function

Estimates of material transfer using Eq. 1 do not fully resolve the coupling between phytoplankton, viruses and microzooplankton. To understand how these fluxes emerge from the coupling between groups, it is necessary to also resolve the production and losses of viruses and grazers, and to explicitly quantify how phytoplankton losses depend on microzooplankton and virus biomass density (Eq. 2). In what follows, we demonstrate how information from dilution experiments and laboratory studies may be combined for a more general prediction of ecosystem structure and function. We begin with a discussion of parameters  $\varphi_v$  and  $\varphi_z$  that constrain the dependence of phytoplankton losses on virus and grazer biomass density. We go on to demonstrate how these parameters can be used to predict ecosystem structure. More general application of these techniques requires direct resolution of the caveats of the dilution technique (Dolan and McKeon, 2005; Baudoux *et al.*, 2006; Kimmanse and Brussaard, 2010; Beckett and Weitz, 2017; Supporting Information Appendix S1C).

#### Comparing maximal clearance rates between viruses and grazers

From Eqs. 1 and 2, maximal carbon clearance rates may be inferred if the virus and grazer biomass density are known:

$$\varphi_v = m_v/V \quad (4)$$

$$\varphi_z = m_z/Z \quad (5)$$

The vast majority of dilution experiments do not measure virus and grazer biomass density, preventing the conversion of loss rates to maximal carbon clearance rates. Yet, Pasulka *et al.* (2015) measured the abundance of viruses as well as the biomass of grazers. We therefore inferred maximal carbon clearance rates in the CCE with Eqs. 4 and 5, using measurements of microzooplankton carbon (Supporting Information Table S2), and the virus abundance data of Pasulka *et al.* (2015). To convert virus abundances to carbon densities, we used the model of Jover *et al.* (2014) (Table 3) to infer virus carbon quota using an assumed virus capsid radius. Algal viruses span a considerable size range, from ~20 nm to 200 nm capsid radius (Brussaard, 2004). A study conducted in the Southern California Bight reported virus particle sizes predominantly towards the lower end of this range, in the majority of cases particle radius was < 40 nm (Cochlan *et al.*, 1993). When a 25 nm capsid radius is assumed, our analysis predicts that biomass normalized viral maximal carbon clearance rates ( $\varphi_v$ ) are higher than grazer maximal carbon clearance rates ( $\varphi_z$ ; Fig. 3A), implying viruses in this system may have a greater propensity (per unit carbon) to kill their hosts than grazers. When 50 nm capsid radius is

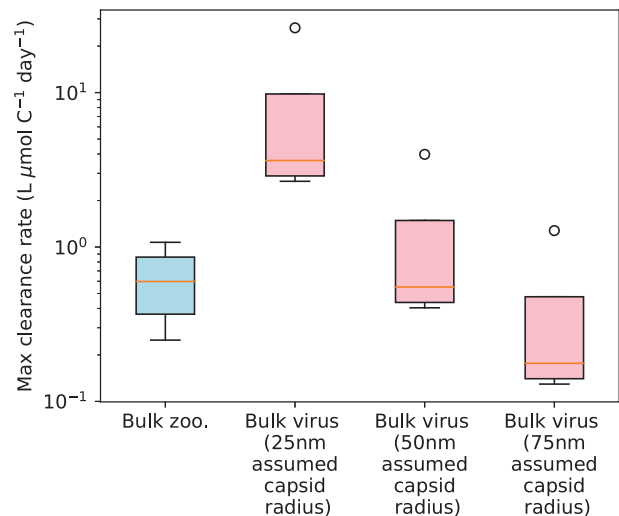


**Fig. 3.** Maximal carbon clearance rates inferred from dilution experiments performed by Pasulka *et al.* (2015). Clearance rates were derived from chlorophyll-a dilution experiments, by normalizing inferred grazer and virus-specific loss rates (units  $\text{day}^{-1}$ ) by bulk grazer and virus biomass ( $\mu\text{mol C l}^{-1}$ ). The data for loss rates, virus abundance and microzooplankton concentration are in Supporting Information Table S2. Upper and lower limits of the boxes are upper and lower quartiles respectively. For viruses, three different estimates of the clearance rate were derived when the capsid radius used to convert from abundance units to carbon units was assumed to be 25, 50 or 75 nm. The analysis shows that the assumed capsid radius has a profound influence on the inferred, carbon-specific viral clearance rate.

assumed, the clearance rates of viruses and grazers are comparable, and when 75 nm radius is assumed, viral maximal carbon clearance rates are smaller than grazer maximal carbon clearance rate (Fig. 3).

It should be emphasized that maximal carbon clearance rates in Fig. 3 are only one component of the realized loss of phytoplankton due to viral lysis and grazing. Estimates of transfer efficiency (Fig. 2) and other constraints on the production and loss of viruses and microzooplankton are important to know the realized rate of transfer. The maximal carbon clearance rate is an important indicator of the propensity for viruses and grazers to capture their prey. Yet, our analysis shows that direct comparisons of maximal carbon clearance rates of viruses and grazers depend critically on measurements of predator and parasite carbon biomass (Fig. 3). Lack of empirical constraint on carbon density makes inference of process-specific model parameters challenging. This limitation could be partially resolved by combining virus particle size with particle concentration measurements to infer virus carbon density.

#### Disentangling taxa-specific from bulk clearance rates

Marine viruses are generally highly hosted species-specific and plankton can exhibit size- and host-selectivity in grazing. Hence, one limitation of using rates inferred from chlorophyll *a* dynamics is the potential to overlook viral (and grazing activity) that occurs only within a subset of the plankton community (Mojica *et al.*, 2016; Beckett and Weitz, 2018). During the same set of dilution treatments, Pasulka *et al.* (2015) inferred viral and grazer loss rates from flow cytometry measurements of *Prochlorococcus* and *Synechococcus*, and also measured the carbon biomass of nanozooplankton grazers. In Supporting Information Appendix S1D and Fig. S4, these measurements were used to predict the maximal carbon clearance rates of nanozooplankton grazers feeding on these cyanobacteria, contrasting also with estimates of cyanophage maximal carbon clearance rates. The analysis shows that, regardless of whether cyanophage is assumed to be 50%, 10% or 1% of the total viral population, cyanophage clearance rates typically exceed nanozooplankton clearance rates (Supporting Information Fig. S1).

Overall, these analyses suggest that robust inference of ecosystem model parameters from community-level experiments requires more detailed measurements of virus community structure to accompany measurements of loss rates.

#### From mechanisms to a simple ecosystem model

We now consider steps required to embed process-specific phytoplankton loss parameters in an ecosystem

and biogeochemical modelling context. Consider a model of material transfer from a phytoplankton community (*P*), to viruses (*V*) and grazers (*Z*):

$$\frac{dP}{dt} = \underbrace{\mu P}_{\text{phyto-growth}} - \underbrace{\varphi_v VP}_{\text{loss due to lysis}} - \underbrace{\varphi_z ZP}_{\text{loss due to grazing}} \quad (6)$$

$$\frac{dV}{dt} = \underbrace{\varepsilon_v \varphi_v VP}_{\text{viral production}} - \underbrace{\delta_{vv} V^2}_{\text{viral losses}} \quad (7)$$

$$\frac{dZ}{dt} = \underbrace{\varepsilon_z \varphi_z ZP}_{\text{grazer production}} - \underbrace{\delta_{zz} Z^2}_{\text{grazer losses}} \quad (8)$$

In Eqs. 7 and 8, the terms  $\varepsilon_v \varphi_v VP$  and  $\varepsilon_z \varphi_z ZP$  are the production of viruses and grazers respectively. We also introduce higher order loss terms,  $\delta_{vv} V^2$  and  $\delta_{zz} Z^2$ . All parameter definitions and units are listed in Table 1. Equations 6–8 place the mass balance in Eq. 2 in a broader ecosystem context, adding only the minimal number of processes to fully resolve the production and losses of phytoplankton, virus and microzooplankton. Producers grow at rate  $\mu$ , and losses due to viral infection and grazing are controlled by linear interaction terms with slopes  $\varphi_v$  and  $\varphi_z$  respectively. The parameters  $\varepsilon_v$  and  $\varepsilon_z$  control the proportion of producer material that is transferred to virus and grazer biomass, and  $\delta_{vv}$  and  $\delta_{zz}$  are virus and grazer mortality parameters respectively.

In Eqs. 7 and 8, we assume virus and microzooplankton losses increase quadratically with virus and grazer biomass density. If losses were assumed to be linear with respect to virus and grazer biomass density, the model leads to competitive exclusion of either the virus or the grazer—a result that is clearly unrealistic, as viruses and grazers coexist throughout the surface ocean. By making loss rates diminish at low biomass density, quadratic mortality promotes coexistence among competing groups. Quadratic increases in loss rates are commonly applied within plankton ecosystem models to mimic the effect of higher trophic levels on the plankton community, implicitly due to increases in the predators of plankton as systems are enriched (Steele and Frost, 1977). Viruses do not form a base in the food chain in the manner that microzooplankton do. Nonetheless, viruses are subject to losses due to particle attachment and grazing (Weinbauer, 2004) and perhaps, for this reason, quadratic loss terms have been shown to characterize viral losses (Middleton *et al.*, 2017). In Supporting Information Appendix S1E, we show that when a linear term is included in Eqs. 6–8, the linear and quadratic

loss parameters have qualitatively similar influence on the steady-state predictions of virus and grazer biomass. We opt to include only the quadratic term for parsimony.

Consider the following steady-state predictions of carbon biomass, found by setting Eqs. 6–8 to zero:

$$P^* = \frac{\mu}{\varepsilon_Z \varphi_Z^2 \left( \frac{\delta_{VV}}{\delta_{ZZ}} \right) + \varepsilon_V \varphi_V^2 \left( \frac{\delta_{ZZ}}{\delta_{VV}} \right)} \quad (9)$$

$$V^* = \frac{\mu \varepsilon_V \varphi_V}{\varepsilon_V \varphi_V^2 + \varepsilon_Z \varphi_Z^2 \left( \frac{\delta_{VV}}{\delta_{ZZ}} \right)} \quad (10)$$

$$Z^* = \frac{\mu \varepsilon_Z \varphi_Z}{\varepsilon_Z \varphi_Z^2 + \varepsilon_V \varphi_V^2 \left( \frac{\delta_{VV}}{\delta_{ZZ}} \right)} \quad (11)$$

Equations 9–11 predict ecosystem biomass structure using community-level life history traits.

#### Modelling ecosystem transfer rates

In Fig. 4A, we show rates of transfer using system-specific loss rates  $m_z$  and  $m_v$ . In Fig. 4B, we show how the ecosystem model can be used to extend these estimates and make predictions about the rate of transfer to each of the fates depicted in Fig. 1. The rates in Fig. 4B were generated by substituting the steady-state solutions from Eqs. 9–11 into the modelled flux terms in Table 2 (Fig. 4B), taking advantage also of our derived estimates of maximal carbon clearance rates  $\varphi_v$  and  $\varphi_z$  (Fig. 3, assuming virus capsid radius 50 nm), and transfer efficiencies  $\varepsilon_v$  and  $\varepsilon_z$  (Fig. 2).

In Table 2, the modelled flux terms all depend linearly on the phytoplankton, virus and microzooplankton

biomass, which in Fig. 4B were assumed to be the steady-state solutions ( $P^*$ ,  $V^*$  and  $Z^*$ ) in Eqs. 9–11. Since all three steady-state solutions in Eqs. 1–3 increase linearly with respect to producer growth rate,  $\mu$ , modelled variation in producer carbon (Fig. 4B) is driven by variation in producer growth rate that we imposed to be consistent with the range observed by Pasulka *et al.* (2015). Furthermore, modelled increases in specific loss rates in Fig. 4B arise due to increases in virus and microzooplankton biomass (Table 2) that also are driven by changes in producer growth rate (Eqs. 10 and 11). The emergent linear relations between specific loss rates and producer carbon in Fig. 4B are qualitatively consistent with relations between dilution based specific loss rates and chlorophyll a concentration in Fig. 4A. These linear relations emerge because of the linear dependence of virus and microzooplankton biomass on producer growth rate in Eqs. 10 and 11, that in turn are a consequence of the coupling between  $P$ ,  $V$  and  $Z$ , in Eqs. 6–8.

The model solutions predict linear relations between phytoplankton biomass and losses to microzooplankton grazers and viruses (Fig. 4B). Yet, the slope of these linear relations depends also on the loss parameters  $\delta_{VV}$  and  $\delta_{ZZ}$  (Eqs. 9–11). In the absence of independent information to constrain higher order loss parameters, we selected values that led to model predictions of  $V^*$  and  $Z^*$  consistent with the observations. In Supporting Information Appendix S1F, we report variation in the residual sum of squares between model predictions of  $V^*$  and  $Z^*$  (Eqs. 9 and 11) and observations of virus and grazer biomass (Pasulka *et al.*, 2015). The sensitivity revealed combinations of  $\delta_{VV}$  and  $\delta_{ZZ}$  that led to good agreement between the model predictions of  $V^*$  and  $Z^*$  and the observations. With values of  $\delta_{VV}$  and

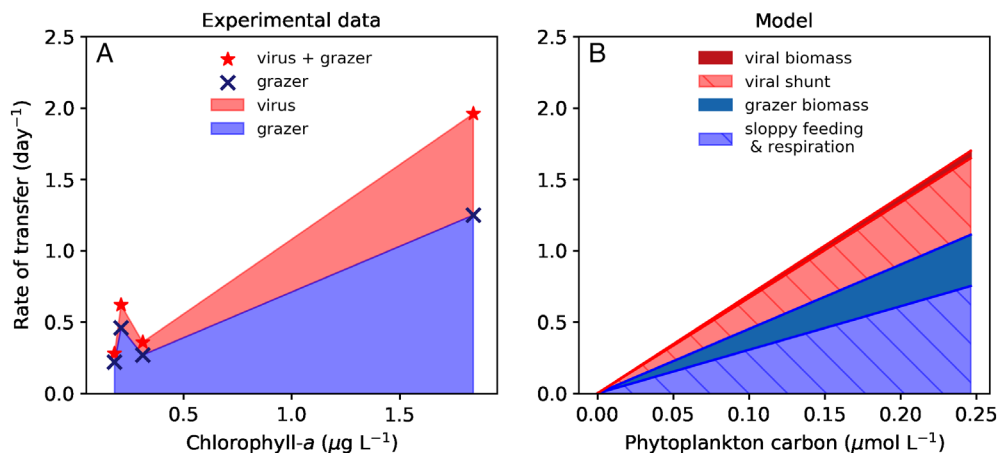


**Fig. 4.** Carbon transfer through viruses and grazers.

A. Dilution based estimates of chlorophyll a loss rates from Pasulka *et al.* (2015).

B. Modelled rates of carbon transfer to grazer biomass, sloppy feeding, excretion and respiration, viruses and viral lysate (referred to in the Figure legend as the 'viral shunt'), using the terms in Table 2, with virus and grazer steady states in Eqs. 5–8. A range of trophic states was simulated by allowing the phytoplankton growth rate to vary within the range [0,1.7] consistent with the measurements of Pasulka *et al.* (2015).

$\delta_{zz}$  guided by this sensitivity (Supporting Information Appendix S1F), we estimate that 19.5%, 40.7%, 1% and 38.8% of total losses flow to grazing, sloppy feeding and respiration, viral biomass and viral lysate respectively. Due to lack of independent constraint on  $\delta_{vv}$  and  $\delta_{zz}$ , we do not attempt to constrain uncertainty on these rate estimates. We note only that the predictions, by design, all fall within the range of estimates based directly on  $m_v$  and  $m_z$  ( $22 \pm 3\%$ ,  $46 \pm 27\%$ ,  $3 \pm 2\%$  and  $29 \pm 20\%$ ).

#### *Towards mechanistic prediction*

Our model estimates of carbon transfer rates are explicit with respect to phytoplankton, virus and grazer biomass, as well as the coupling between these pools (Fig. 4B). Yet, they do not add constraint to estimates of the same fluxes using  $m_v$  and  $m_z$  directly from dilution experiments (Fig. 4A). Indeed, inclusion of the additional parameters  $\delta_{vv}$  and  $\delta_{zz}$  adds uncertainty. Nevertheless, by incorporating ecosystem feedbacks and the steady-state solutions in Eqs. 9–11, the predictions are based on the coupling between phytoplankton producers, parasites and predators, and could be integrated within biogeochemical and carbon cycle models. Furthermore, they may be used to examine mechanistic constraints on carbon flow. For example, the CCE estimated phytoplankton loss rate due to grazing is higher than it is to viral lysis (Fig. 4A). Our analysis reveals that these high loss rates may be due to high transfer efficiency of carbon to grazers by comparison to viruses (Fig. 2). Clear differences in transfer efficiency are likely to confer advantages to grazers, even when their maximal carbon clearance rates are comparable or lower by comparison to viruses (Fig. 3). This analysis demonstrates how maximal clearance rates and transfer efficiencies may be combined for more general, prognostic understanding of ecosystem carbon transfer rates. If uncertainties associated with the dilution technique can be resolved (Beckett and Weitz, 2017, 2018, see also Supporting Information Appendix S1C: *Caveats and Limitations*), these approaches will enable broader parameterization of ecosystem carbon fluxes.

#### *Model caveats and limitations*

Our ecosystem model considers phytoplankton, viruses and microzooplankton each as homogeneous biomass pools, and disregards group-, species- and strain-specific interactions that may fundamentally influence ecosystem structure and function (Thingstad, 2000; Le Quere *et al.*, 2005; Follows *et al.*, 2007; Friedrichs *et al.*, 2007; Våge *et al.*, 2013, 2018; Thingstad *et al.*, 2014; Weitz *et al.*, 2015). Viral infection and grazing rates are treated with Holling I encounter terms, overlooking the potential for

grazing rate to saturate with prey density, consistent with the Holling II functional response (Holling, 1959). A third type of response, with a sigmoidal shape as a function of resource concentration, was observed by Holling (1959), and has been found in a range of zooplankton groups (Steele and Frost, 1977; Jeschke *et al.*, 2004), and alternative functional forms have been proposed linking key response parameters to allometry (Flynn and Mitra, 2016) and behaviour-based prey selectivity (Weisse *et al.*, 2016). We limited our attention to Holling I, and neglected group, species or strain level interactions, to demonstrate how carbon flow can be quantitatively constrained with existing field and laboratory data. Our goal was to motivate more detailed empirical, quantitative model constraint.

A major source of uncertainty in our model predictions is due to lack of constraint on the virus and grazer loss processes, which are encapsulated in the parameters  $\delta_{vv}$  and  $\delta_{zz}$ . We assumed quadratic losses since this enabled microzooplankton and viruses to coexist. An alternative way for models to maintain coexistence among viruses and microzooplankton grazers is to allow the different groups to persist by feeding in parallel on groups within the producer community that have different rates of resource uptake and susceptibility to predation (Thingstad and Lignell, 1997; Våge *et al.*, 2013). We acknowledge the value of explicit resolution of diverse plankton traits for mechanistic resolution of community dynamics. To this end, we advocate for more widespread measurement of group-specific phytoplankton growth and loss processes (Mojica *et al.*, 2016), combined with measurements of carbon-density within different groups.

#### **Summary and conclusions**

For decades, dilution experiments have been routinely used to quantify phytoplankton and cyanobacteria losses due to microzooplankton grazing (Landry and Hassett, 1982; Calbet and Landry, 2004). More recently, the modified dilution assay has been used for phytoplankton viral lysis rate measurements (Evans *et al.*, 2003; Kimmance and Brussaard, 2010). The modified dilution technique has been implemented in diverse environments, ranging for example through trophic gradients of the Pacific and Atlantic gyres (Pasulka *et al.*, 2015; Mojica *et al.*, 2016), to continental shelf and coastal environments including the western English Channel and the North Sea (Kimmance *et al.*, 2007; Baudoux *et al.*, 2008) and coastal Taiwan (Tsai *et al.*, 2012). A view is beginning to emerge of viral lysis and grazing both contributing appreciably to total phytoplankton losses. For example, viral lysis of picoeukaryotic groups in the North Sea ranged from insignificant, to  $0.23 \text{ day}^{-1}$ , whereas grazing by



microzooplankton was typically between 0.2 and 0.4 day<sup>-1</sup> (Baudoux *et al.*, 2008). Mojica *et al.* (2016) found equivalent impact of viral lysis and grazing at low latitudes in the North Atlantic, shifting to grazer dominated losses further north.

Despite the progress that has been made, it is still unclear how viral infection and grazing influence nutrient turnover and carbon sequestration within marine systems. We have shown steps necessary to embed community-level measurements within biogeochemical models to allow assessment of virus and grazer impacts on carbon flow on broad-scales. We used a single dataset from the CCE, as this was the only instance we could find of virus and grazer abundance measurements taken collectively with dilution experiments (Pasulka *et al.*, 2015). These data were used to quantitatively constrain the dependence of viral lysis and grazing on virus and grazer biomass density, within mixed plankton communities. Data from the CCE were augmented with estimates of transfer efficiencies from laboratory experiments. Empirical constraint on the density dependence of lysis and grazing and transfer efficiency are important steps for more general, empirical constraint on the 'viral shunt' (Wilhelm and Suttle, 1999) within models. For the CCE, we estimate that of the combined losses due to grazing and viral lysis, 22 ± 3%, 46 ± 27%, 3 ± 2% and 29 ± 20% go to grazers, sloppy feeding and respiration, viral biomass and viral lysate respectively.

For more widespread empirical constraint on ecosystem models, it would be best for dilution experiments to more routinely be accompanied with measurements of phytoplankton, virus and grazer biomass density (including also virus and grazer size and composition). Doing so would lead to reduced uncertainty on estimates of carbon flux and allow far greater synergy between observational findings and ecosystem models. As variants of the dilution technique are explored, model formulations can be altered and expanded to describe additional processes, such as species or strain-specific diversity of growth and losses (Thingstad, 2000; Våge *et al.*, 2013; Beckett and Weitz, 2018), trade-offs (Thingstad *et al.*, 2014; Record *et al.*, 2016) and nonlinear interaction terms (Li *et al.*, 2017; Sandhu *et al.*, 2018; see also Supporting Information Appendix S1G). Closer interaction between experimental manipulations and model parameterization may open the door to deeper understanding of microbial ecosystem impacts on carbon transfer at global scales.

### Acknowledgements

Talmy and Follows acknowledge NSF Biological Oceanography grant 1536521. Follows and Weitz acknowledges

support from the Simons Foundation (SCOPE Award ID 329108). Follows also acknowledges Simons Collaboration CBIOMES Award 549931.

### References

- Baudoux, A.-C., Noordeloos, A.A.M., Veldhuis, M.J.W., and Brussaard, C.P.D. (2006) Virally induced mortality of *Phaeocystis globosa* during two spring blooms in temperate coastal waters. *Aquat Microb Ecol* **44**: 207–217.
- Baudoux, A.C., Veldhuis, M.J.W., Noordeloos, A.A.M., Van Noort, G., and Brussaard, C.P.D. (2008) Estimates of virus- vs. grazing induced mortality of picophytoplankton in the North Sea during summer. *Aquat Microb Ecol* **52**: 69–82.
- Beckett, S.J., and Weitz, J.S. (2017) Disentangling niche competition from grazing mortality in phytoplankton dilution experiments. *PLoS One* **12**: e0177517.
- Beckett, S.J., and Weitz, J.S. (2018) The effect of strain level diversity on robust inference of virus-induced mortality of phytoplankton. *Front Microbiol* **9**: 1–15.
- Breitbar, M., Bonnain, C., Malki, K., and Sawaya, N.A. (2018) Phage puppet masters of the marine microbial realm. *Nat Microbiol* **3**: 1.
- Brum, J.R., Hurwitz, B.L., Schofield, O., Ducklow, H.W., and Sullivan, M.B. (2015) Seasonal time bombs: dominant temperate viruses affect Southern Ocean microbial dynamics. *ISME J* **10**: 437–449.
- Brussaard, C.P.D. (2004) Viral control of phytoplankton populations—a review. *J Eukaryot Microbiol* **51**: 125–138.
- Brussaard, C.P.D., Wilhelm, S.W., Thingstad, F., Weinbauer, M.G., Bratbak, G., Haldal, M., *et al.* (2008) Global-scale processes with a nanoscale drive: the role of marine viruses. *ISME J* **2**: 575–578.
- Calbet, A., and Landry, M.R. (2004) Phytoplankton growth, microzooplankton grazing, and carbon cycling in marine systems. *Limnol Oceanogr* **49**: 51–57.
- Chen, B., Laws, E.A., Liu, H., and Huang, B. (2014) Estimating microzooplankton grazing half-saturation constants from dilution experiments with nonlinear feeding kinetics. *Limnol Oceanogr* **59**: 639–644.
- Cochlan, W.P., Wikner, J., Steward, G.F., Smith, D.C., and Azam, F. (1993) Spatial distribution of viruses, bacteria and chlorophyll *a* in neritic, oceanic and estuarine environments. *Mar Ecol Prog Ser* **92**: 77–87.
- Dolan, J.R., and McKeon, K. (2005) The reliability of grazing rate estimates from dilution experiments: have we overestimated rates of organic carbon consumption? *Ocean Sci Discuss* **1**: 21–36.
- Engel, A., Thoms, S., Riebesell, U., Rochelle-Newall, E., and Zondervan, I. (2004) Polysaccharide aggregation as a potential sink of marine dissolved organic carbon. *Nature* **428**: 929–932.
- Evans, C., and Brussaard, C.P.D. (2012) Regional variation in lytic and lysogenic viral infection in the Southern Ocean and its contribution to biogeochemical cycling. *Appl Environ Microbiol* **78**: 6741–6748.
- Evans, C., Archer, S.D., Jacques, S., and Wilson, W.H. (2003) Direct estimates of the contribution of viral lysis and microzooplankton grazing to the decline of a *Micromonas* spp. population. *Aquat Microb Ecol* **30**: 207–219.

- Flynn, K.J., and Mitra, A. (2016) Why plankton modelers should reconsider using rectangular hyperbolic (Michaelis-Menten, Monod) descriptions of predator-prey interactions. *Front Mar Sci* **3**: 165. <https://doi.org/10.3389/fmars.2016.00165>.
- Follows, M.J., Dutkiewicz, S., Grant, S., and Chisholm, S.W. (2007) Emergent biogeography of microbial communities in a model ocean. *Science* (80-. ) **315**: 1843–1846.
- Friedrichs, M.A.M., Dusenberry, J.A., Anderson, L.A., Armstrong, R.A., Chai, F., Christian, J.R., et al. (2007) Assessment of skill and portability in regional marine biogeochemical models: role of multiple planktonic groups. *J Geophys Res* **112**: 1–22.
- Fuhrman, J.A. (1999) Marine viruses and their biogeochemical and ecological effects. *Nature* **399**: 541–548.
- Guidi, L., Chaffron, S., Bittner, L., Eveillard, D., Larhlimi, A., Roux, S., et al. (2015) Plankton networks driving carbon export in the oligotrophic ocean. *Nature* **532**: 465–470.
- Holling, C.S. (1959) The components of predation as revealed by a study of small-mammal predation of the European pine sawfly. *Can Entomol* **91**: 293–320.
- Jeschke, J.M., Kopp, M., and Tollrian, R. (2004) Consumer-food systems: why type I functional responses are exclusive to filter feeders. *Biol Rev* **79**: 337–349.
- Jover, L.F., Effler, T.C., Buchan, A., Wilhelm, S.W., and Weitz, J.S. (2014) The elemental composition of virus particles: implications for marine biogeochemical cycles. *Nat Rev Microbiol* **12**: 519–528.
- Kimmance, S.A., and Brussaard, C.P.D. (2010) Estimation of viral-induced phytoplankton mortality using the modified dilution method. In *Manual of Aquatic Viral Ecology*, Wilhelm, S.W., Weinbauer, M.G., and Suttle, C.A. (eds). Waco, TX: American Society of Limnology and Oceanography Inc., pp. 65–73.
- Kimmance, S.A., Wilson, W.H., and Archer, S.D. (2007) Modified dilution technique to estimate viral versus grazing mortality of phytoplankton: limitations associated with method sensitivity in natural waters. *Aquat Microb Ecol* **49**: 207–222.
- Kjørboe, T. (2011) How zooplankton feed: mechanisms, traits and trade-offs. *Biol Rev* **86**: 311–339.
- Laber, C.P., Hunter, J.E., Carvalho, F., Collins, J.R., Hunter, E.J., Schieler, B.M., et al. (2018) Coccolithovirus facilitation of carbon export in the North Atlantic. *Nat Microbiol* **3**: 537–547.
- Landry, M.R., and Hassett, R.P. (1982) Estimating the grazing impact of marine micro-zooplankton. *Mar Biol* **67**: 283–288.
- Le Quere, C., Harrison, S.P., Prentice, I.C., Buitenhuis, E.T., Aumont, O., Bopp, L., et al. (2005) Ecosystem dynamics based on plankton functional types for global ocean biogeochemistry models. *Glob Chang Biol* **11**: 2016–2040.
- Li, Q.P., Franks, P.J.S., and Landry, M.R. (2011) Microzooplankton grazing dynamics: parameterizing grazing models with dilution experiment data from the California current ecosystem. *Mar Ecol Prog Ser* **438**: 59–69.
- Li, Q.P., Franks, P.J.S., and Landry, M.R. (2017) Recovering growth and grazing rates from nonlinear dilution experiments. *Limnol Oceanogr* **62**: 1825–1835.
- Menden-Deuer, S., and Lessard, E.J. (2000) Carbon to volume relationships for dinoflagellates, diatoms, and other protist plankton. *Limnol Oceanogr* **45**: 569–579.
- Middleton, J.E., Martínez Martínez, J., Wilson, W.H., and Record, N.R. (2017) Functional dynamics of *Emiliania huxleyi* virus-host interactions across multiple spatial scales. *Limnol Oceanogr* **62**: 922–933.
- Mojica, K.D.A., Huisman, J., Wilhelm, S.W., and Brussaard, C. P.D. (2016) Latitudinal variation in virus-induced mortality of phytoplankton across the North Atlantic Ocean. *ISME J* **10**: 500–513.
- Pasulka, A.L., Samo, T.J., and Landry, M.R. (2015) Grazer and viral impacts on microbial growth and mortality in the southern California current ecosystem. *J Plankton Res* **37**: 1–17.
- Record, N.R., Talmy, D., and Vage, S. (2016) Quantifying tradeoffs for marine viruses. *Front Mar Sci* **3**: 1–27.
- Sandhu, S.K., Morozov, A.Y., Mitra, A., and Flynn, K. (2018) Exploring nonlinear functional responses of zooplankton grazers in dilution experiments via optimization techniques. *Limnol Oceanogr* **9999**: 1–11.
- Steele, J.H., and Frost, B.W. (1977) The structure of plankton communities. *Philos Trans R Soc Lond B Biol Sci* **280**: 485–534.
- Stukel, M.R., Landry, M.R., Benitez-nelson, C.R., and Goericke, R. (2011) Trophic cycling and carbon export relationships in the California current ecosystem. *Limnol Oceanogr* **56**: 1866–1878.
- Taniguchi, D.A.A., Franks, P.J.S., and Poulin, F.J. (2014) Planktonic biomass size spectra: an emergent property of size-dependent physiological rates, food web dynamics, and nutrient regimes. *Mar Ecol Prog Ser* **514**: 13–33.
- Thingstad, T.F. (2000) Elements of a theory for the mechanisms controlling abundance, diversity, and biogeochemical role of lytic bacterial viruses in aquatic systems. *Limnol Oceanogr* **45**: 1320–1328.
- Thingstad, T.F., and Lignell, R. (1997) Theoretical models for the control of bacterial growth rate, abundance, diversity and carbon demand. *Aquat Microb Ecol* **13**: 19–27.
- Thingstad, T.F., Våge, S., Storesund, J.E., Sandaa, R.A., and Giske, J. (2014) A theoretical analysis of how strain-specific viruses can control microbial species diversity. *Proc Natl Acad Sci USA* **111**: 7813–7818.
- Tsai, A.Y., Gong, G.C., Sanders, R.W., Chiang, K.P., Huang, J. K., and Chan, Y.F. (2012) Viral lysis and nanoflagellate grazing as factors controlling diel variations of *Synechococcus* spp. summer abundance in coastal waters of Taiwan. *Aquat Microb Ecol* **66**: 159–167.
- Våge, S., Storesund, J.E., and Thingstad, T.F. (2013) Adding a cost of resistance description extends the ability of virus-host model to explain observed patterns in structure and function of pelagic microbial communities. *Environ Microbiol* **15**: 1842–1852.
- Våge, S., Bratbak, G., Egge, J., Heldal, M., Larsen, A., Norland, S., et al. (2018) Simple models combining competition, defence and resource availability have broad implications in pelagic microbial food webs. *Ecol Lett* **21**: 1440–1452.
- Weinbauer, M.G. (2004) Ecology of prokaryotic viruses. *FEMS Microbiol Rev* **28**: 127–181.
- Weisse, T., Anderson, R., Arndt, H., Calbet, A., Hansen, P. J., and Montagnes, D.J.S. (2016) Functional ecology of aquatic phagotrophic protists—concepts, limitations, and perspectives. *Eur J Protistol* **55**: 50–74.

- Weitz, J.S. (2015) *Quantitative Viral Ecology: Dynamics of Viruses and their Microbial Hosts*. Princeton, NJ: Princeton University Press.
- Weitz, J.S., and Wilhelm, S.W. (2012) Ocean viruses and their effects on microbial communities and biogeochemical cycles. *F1000 Biol Rep* **4**: 17.
- Weitz, J.S., Stock, C.A., Wilhelm, S.W., Bourouiba, L., Coleman, M.L., Buchan, A., *et al.* (2015) A multitrophic model to quantify the effects of marine viruses on microbial food webs and ecosystem processes. *ISME J* **9**: 1352–1364.
- Wilhelm, S.W., and Suttle, C.A. (1999) Viruses and nutrient cycles the sea. *Bioscience* **49**: 781–788.

### Supporting Information

Additional Supporting Information may be found in the online version of this article at the publisher's web-site:

**Appendix S1:** Supporting Information. A) Estimating maximal clearance rates from dilution experiments. B) Model Uncertainty. C) Caveats and limitations of the dilution technique. D) Resolving maximal clearance rates in diverse communities. E) Holling II saturation parameters from dilution experiments. F) Model with linear and quadratic closure terms.

**Table S1.** Virus gross growth efficiency (GGE,  $\epsilon_v$ ) reference material. Allometric relations in Table were used to convert from particle and cell radius to carbon content, in each case assuming spherical shape. Data for virus GGEs ( $\epsilon_v$ ) are shown in Fig. 2.

**Table S2.** Loss rates, virus abundance, and zooplankton carbon biomass in the California Current from Pasulka *et al.* (2015). *Prochlorococcus* were not detected in Experiment 3. Picoeukaryotes were sorted by Pasulka *et al.* (2015) but were scarce by comparison to *Prochlorococcus* and *Synechococcus* and are neglected here.